Mon. Not. R. astr. Soc. (1968) **141**, 445–458.

ON COSMOLOGICAL MODELS WITH AN ANTIPOLE

M. Rowan-Robinson

(Received 1968 May 1)

Summary

The properties of Lemaître models are summarized and the luminosity–volume test is used to determine which of these models are consistent with the distributions in space of quasars and radio-galaxies respectively. Ranges of models can be found consistent with either, but not both, of these classes of radio-source, including models which could account for the anomalous absorption redshift of 1·95 in quasars. The integrated extragalactic radio background provides an important additional constraint to the problem. No model is found to agree with the observed radio source-counts, without the introduction of evolutionary effects.

1. *Introduction.* If the redshifts of quasars are cosmological, their distribution in space is inconsistent with a wide range of cosmological models (**1**)–(**3**). The distribution in space of galaxies identified with radio-sources in the 3C catalogue also appears to be inconsistent with relativistic cosmological models having $0 \leqslant \sigma_0 \leqslant 3$, $-1 \leqslant q_0 \leqslant 3$, where $\sigma_0 = 4\pi G\rho_0/H_0^2$, $q_0 = -(R\ddot{R}/\dot{R}^2)_0$, $H = (\dot{R}/R)_0$, $R(t)$ is the scale-factor of the expanding universe and the subscript zero refers to the present epoch (**4**).

Consistency of both quasars and radio-galaxies with such models can be achieved by supposing that the co-moving coordinate number-density of sources, or their luminosity, or both, have a negative exponential dependence on the scale factor, $R(t)$ (**4**).

An alternative approach is to consider the more unusual models associated with the name of Lemaître, in which there is the possibility of an antipole (**5**)–(**9**). In addition to the possibility of accounting for the distribution of quasars and radio-galaxies in space, these models can provide a cosmological explanation of the anomalous absorption redshift reported by Burbidge & Burbidge (**10**). Indeed, Shklovsky (**6**) has suggested that this anomalous absorption redshift is one of the strongest pieces of evidence that the redshifts of quasars are cosmological. Solheim (**9**) has suggested a further possible piece of evidence in favour of models with an antipole, that there exists a positive correlation between radio-sources in the 4C catalogue in opposite directions in the sky.

In this paper the luminosity–volume test (**2**), (**4**) is used to determine which cosmological models are consistent with the distributions in space of the quasars and of the radio-galaxies. Important additional constraints are provided by the radio source-counts to low flux-level and the integrated extra galactic radio background at 178 MHz.

2. *Properties of Lemaître models.* For homogeneous, isotropic, pressure-free cosmological models, Einstein's equations reduce to

$$\Lambda/3 = (\sigma_0 - q_0)H_0^2$$
$$kc^2/R_0^2 = (3\sigma_0 - q_0)H_0^2$$

where, for Lemaître models, $\Lambda > 0$ and $k = +1$. Thus

$$\Lambda = \Lambda_c(1+\epsilon) \qquad \text{where} \qquad \Lambda_c = (c^3/4\pi G\rho_0 R_0^3)^2 \tag{1}$$

and

$$1+\epsilon = \frac{27\sigma_0^2(\sigma_0 - q_0)}{(3\sigma_0 - q_0 - 1)^3}. \tag{2}$$

If $\epsilon = 0$ and $Z = (3\sigma_0 - q_0 - 1)/3\sigma_0 = Z_m$, where $Z = 1+z = R_0/R$ and z is the redshift, then $\dot{R} = 0$, $\ddot{R} = 0$ and the universe is static with cosmological repulsion just balancing gravity. If $0 < Z_m < 1$, this state is attained as $t \to \infty$, and if $1 < Z_m$, the universe expanded out of this state at $t = -\infty$.

If $\epsilon > 0$, $Z_m > 1$, the scale-factor, $R(t)$, passes through a point of inflection at an epoch given by $Z = Z_m(1+\epsilon)^{1/3}$. If $0 < \epsilon \ll 1$, the universe 'stagnates' near this point of inflection with $Z \simeq Z_m$.

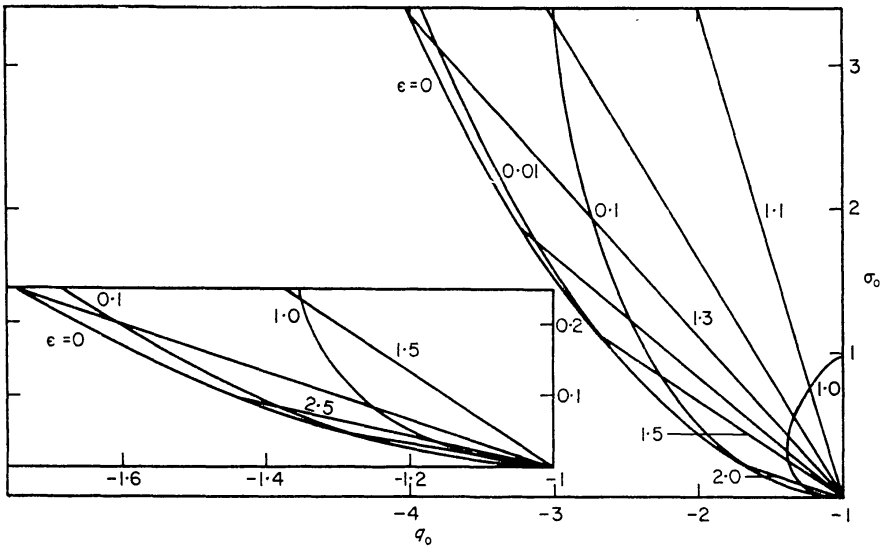

FIG. 1. σ_0–q_0, *the model diagram, showing lines of constant* Z_m *and* ϵ. *The straight lines radiating from* $(\sigma_0, q_0) = (0, -1)$ *are lines of constant* Z_m. *The curved lines are* $\epsilon = 0$, 0·01, 0·1, 1·0. *A portion of the diagram near* $(\sigma_0, q_0) = (0, -1)$ *is shown enlarged (inset).*

Using equations (1) and (2),

$$\sigma_0 = 1/\{Z_m^3(1+\epsilon) + 2 - 3Z_m\} \tag{3}$$

$$q_0 = (1 - Z_m^3(1+\varepsilon))/\{Z_m^3(1+\epsilon) + 2 - 3Z_m\} \tag{4}$$

so

$$1 + q_0 = -3\sigma_0(Z_m - 1).$$

Lines of constant Z_m and ϵ in the $\sigma_0 - q_0$ plane are shown in Fig. 1; the lines of constant Z_m are straight lines radiating from $(0, -1)$. The contribution of observed material in galaxies to ρ_0 is estimated by Oort (**15**) as 7×10^{-31} g cm^{-3}. Thus $\sigma_0 \geqslant 0{\cdot}035$, and from equation (3), $Z_m \leqslant 3{\cdot}3$. We see that $Z_m > 1$ implies $q_0 < -1$, in contradiction to the evidence from the brightest galaxies in clusters (**16**). However, Tinsley (**17**) has recently shown that effects of galactic evolution would be more pronounced in models with $q_0 < -1$, so that they can be reconciled with the observations.

3. *Cosmological explanations of the anomalous absorption redshift at* 1·95

3.1 If $0<\epsilon\ll 1$, photons from sources with $Z>Z_m$ (>1) spend a large part of their travel-time traversing material with $Z\simeq Z_m$ (**6**). Using the fact that the anomalous absorption redshifts of quasars satisfy $z=1{\cdot}95\pm 0{\cdot}01$ (**10**), Kardashev (**7**) calculates that $\epsilon=2.10^{-5}$. Actually there is a slight error in this calculation since the optical depth

$$\tau(z)=\bar{n}_0\bar{\Sigma}_0\int_1^{1+z}\frac{Z^3.Rdr}{1+\frac{1}{4}kr^2}$$

where $\bar{n}_0$ is the average particle density, and $\bar{\Sigma}_0$ the average cross-section at the present epoch. Thus

$$\tau(z)=n_0\bar{\Sigma}_0R_0\int_1^{1+z}\frac{Z^2dZ}{Q}$$

$$Q=\left\{\frac{\sigma_0-q_0+(1+q_0-3\sigma_0)Z^2+2\sigma_0Z^3}{3\sigma_0-q_0-1}\right\}^{1/2}$$

$$=\{\tfrac{2}{3}Z^3Z_m^{-1}+\tfrac{1}{3}Z_m^2(1+\epsilon)-Z^2\}^{1/2},$$

using equations (3) and (4). Kardashev (**7**) has a factor $(1+\epsilon)$ multiplying the first term in the bracket (also an incorrect sign for the third term, which is presumably a printing error, since it appears correctly in the Russian version of this letter, in *Astr. Zirk.*, **430** (1967)). His equation (10) should then read

$$\epsilon=3Q_m^2/(1+z_m)^2=6\times 10^{-5}.$$

However, since ϵ depends on the square of the dispersion in the absorption redshift and also on the square of the quantity $\bar{n}_0\bar{\Sigma}_0$, a factor of 3 is not too relevant.

3.2 A further consequence of the stagnation of the universe near $Z=Z_m$ is that the photons from a distant source may have time to make a complete circuit of the closed universe.

The luminosity distance, D, defined by

$$\mathscr{F}=\mathscr{f}+2\log_{10}D(z)-0{\cdot}4K(z) \qquad (6)$$

where $\mathscr{F}=\log_{10}P$; P is the monochromatic luminosity

$\mathscr{f}=\log_{10}S$; S is the monochromatic flux

and $K(z)$ is the K-correction (see, for example, Appendix 1 of Ref. (**2**)), is given by

$$D(z)=R_0Z\sin\chi(z)$$

where

$$\sin\chi(z)=r/(1+\tfrac{1}{4}kr^2)$$

and

$$\chi(z)=\int_1^{1+z}\frac{dZ}{Q}.$$

Thus

$$\frac{\partial\chi}{\partial\epsilon}=-\frac{1}{2}\int_1^{1+z}\frac{Z_m^2}{3Q^3}dZ<0$$

and in fact $\chi(z)\to\infty$ as $\epsilon\to 0$ if $1+z\geqslant Z_m$. Sources such that $\chi(z)$ is an integral

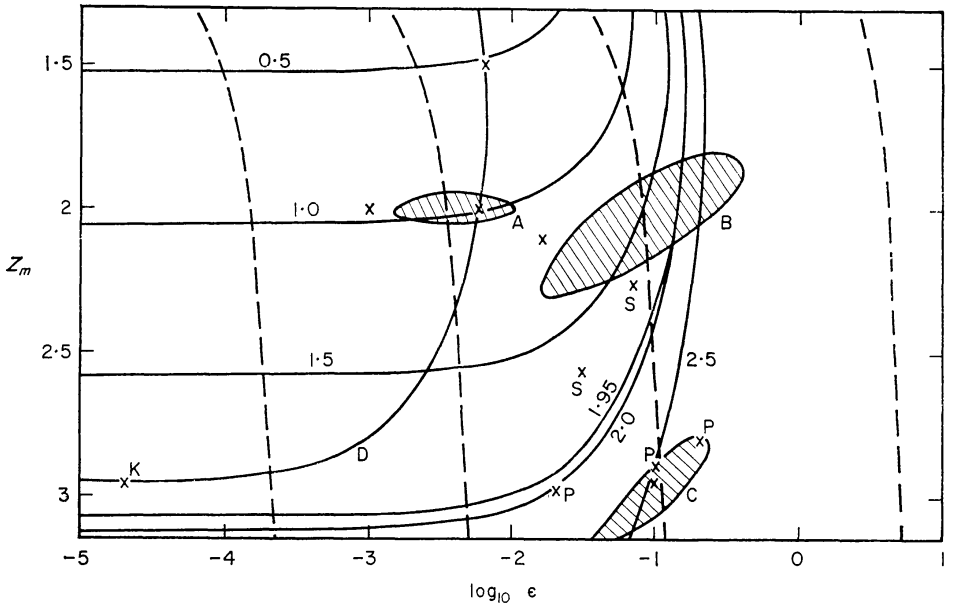

FIG. 2. *Z_m–ϵ. The four broken lines correspond from right to left to $\chi(\infty) = \pi, 2\pi, 3\pi, 4\pi$ respectively. The continuous line labelled D is the locus $\chi(1{\cdot}95) = 2\pi$. The other continuous lines are $\chi(z) = \pi$, where $z = 0{\cdot}5, 1{\cdot}0, 1{\cdot}5, 1{\cdot}95, 2{\cdot}0, 2{\cdot}5$. The shaded areas A,B, C denote models consistent with the distribution in space of the quasars. Crosses denote particular models advocated by various authors (P = Petrosian, Salpeter & Szekeres: S = Solheim: K = Kardashev) and other particular models discussed in this paper.*

multiple of π appear to be infinitely bright. The light from a source at redshift such that $\chi(z) > \pi$ passes through a single point, the antipole. If $\chi(z) > 2\pi$, photons will have passed the observer at an earlier epoch. Thus if sufficiently opaque material is situated at the antipole, or if such material existed in the vicinity of the Earth at an earlier epoch, absorption lines displaced by the corresponding redshifts would be produced.*

The requirement is rather severe,

$$n\Sigma \sim \bar{n}_0 \bar{\Sigma}_0 \cdot \frac{20c}{H_0 L}$$

where L is the dimension of the opaque region. Thus for a region of galactic dimensions, $L \sim 10^5$ light years, $n\Sigma \sim 2 \cdot 10^6 \bar{n}_0 \bar{\Sigma}_0$.

Fig. 2 shows the loci $\chi(\infty) = \pi, 2\pi, 3\pi, 4\pi$ in the $Z_m - \epsilon$ plane. No antipole occurs in models to the right of the $\chi(z) = \pi$ curve. Also shown are the loci of models such that $\chi(z) = \pi$ for $z = 0{\cdot}5, 1, 1{\cdot}5, 2, 2{\cdot}5$ and such that $\chi(1{\cdot}95) = \pi, 2\pi$. The latter two loci give models that could explain the anomalous absorption redshift of 1·95 by method (b). The line of models $Z_m = 2{\cdot}95$ corresponds to method (a).

4. *Luminosity–volume test.* If the fraction of material in the form of sources in a given range of luminosity is independent of epoch, then the distribution of such sources should be uniform with respect to coordinate volume, $V(z)$, where

$$V(z) = \int_0^z \frac{4\pi r^2 dr}{(1 + \frac{1}{4}kr^2)^3}$$

$$= 2\pi(\chi - \sin\chi \cos\chi).$$

* This suggestion was made to me by J. Solheim and M. Rees.

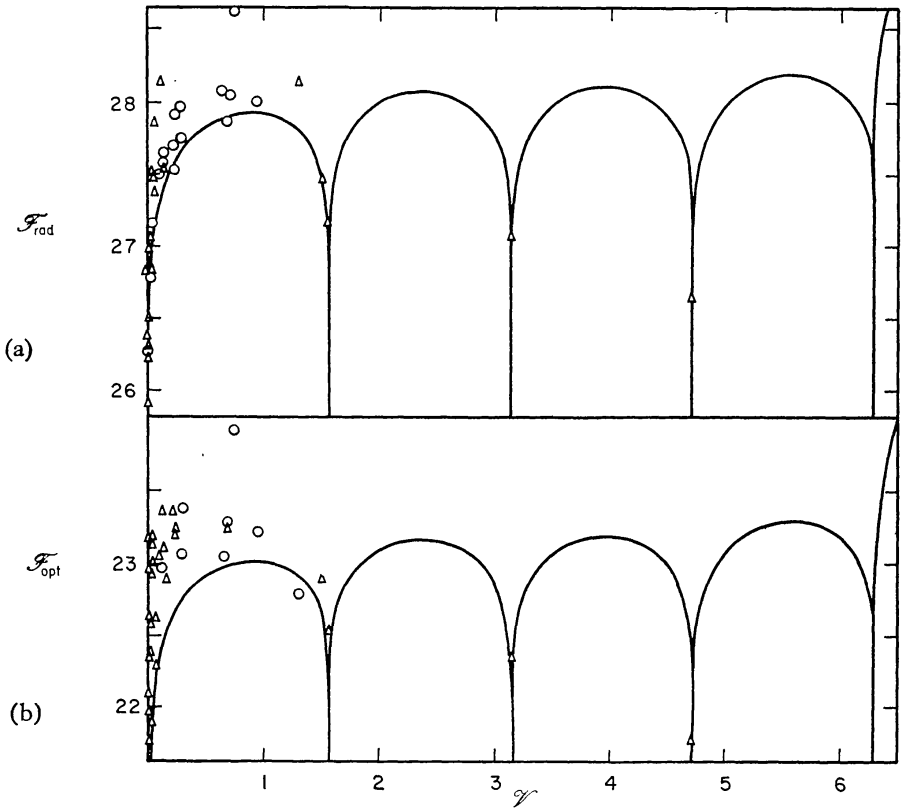

FIG. 3. *The distribution of* (*a*) *radio and* (*b*) *optical, luminosities of* 3*C quasars against volume for the model* $Z_m = 2{\cdot}95$, $\epsilon = 0{\cdot}00002$. *In Fig.* 3(*a*), *circles denote sources with* $\mathcal{F}_{\text{opt}} \geqslant \mathcal{F}_1 = 23{\cdot}05$; *triangles denote sources with* $\mathcal{F}_{\text{opt}} < \mathcal{F}_1$. *In Fig.* 3(*b*), *circles denote sources with* $\mathcal{F}_{\text{rad}} \geqslant \mathcal{F}_2 = 27{\cdot}95$; *triangles denote sources with* $\mathcal{F}_{\text{rad}} < \mathcal{F}_2$. *The units of luminosity are* $w(c/s)^{-1}$ *ster*$^{-1}$ (*and* $\mathcal{F} = \log_{10} P$). *The continuous curves denote the cut-offs imposed by the limiting* 3*C flux-level of* $9{\cdot}10^{-26}$ $w\,m^{-2}(c/s)^{-1}$ *and by the limiting visual magnitude of about* 19 *for quasars, respectively.*

4.1 *Quasars.* The distributions of radio and optical luminosities of quasars against volume are shown in Fig. 3(a), (b) for the model proposed by Kardashev. The data used is that given in Table I of Ref. (**2**) and the luminosities are calculated from equation (6) above. The effect of the limiting 3C flux-level of 9.10^{-26} w m^{-2} (c/s)$^{-1}$ is shown by the continuous curve in Fig. 3(a), and the limit $V = 19$ magnitudes in Fig. 3(b). The radio/optical distribution may be corrected for the effect of optical/radio selection by confining attention to sources with higher optical/radio luminosity, i.e. those denoted by a circle. The distributions are strikingly non-uniform.

On the other hand in the model with $Z_m = 2{\cdot}95$, $\epsilon = 0{\cdot}1$, which is close to one of those advocated by Petrosian, Salpeter & Szekeres (**5**), the distributions are comparatively uniform (Fig. 4(a), (b)). However, since the antipole occurs at redshift (z) 2·58, sources of high flux-density ought to be visible corresponding to this remoter epoch. Some additional hypothesis would be needed to explain the absence of these, for example the gravitational defocusing action of inhomogeneities (**5**).* Models in the shaded regions B and C of Fig. 2 fall into this category.

* Although the condition for this effect to be significant, that an appreciable fraction of the material in the universe be condensed into galaxies, may not be satisfied at the early epochs corresponding to these large redshifts.

Still more satisfactory are a range of models with $Z_m = 2{\cdot}0$. The radio and optical luminosity-volume diagrams for that with $\epsilon = 0{\cdot}0056$, in which

$$\chi(1{\cdot}95) = 2\pi,$$

are shown in Fig. 5(a), (b). In this model and those which fall in the shaded region A of Fig. 2, the corrected optical and radio distributions are uniform with respect to volume; a natural explanation is provided of the absence of quasars in 3C with redshifts greater than about 2·2.

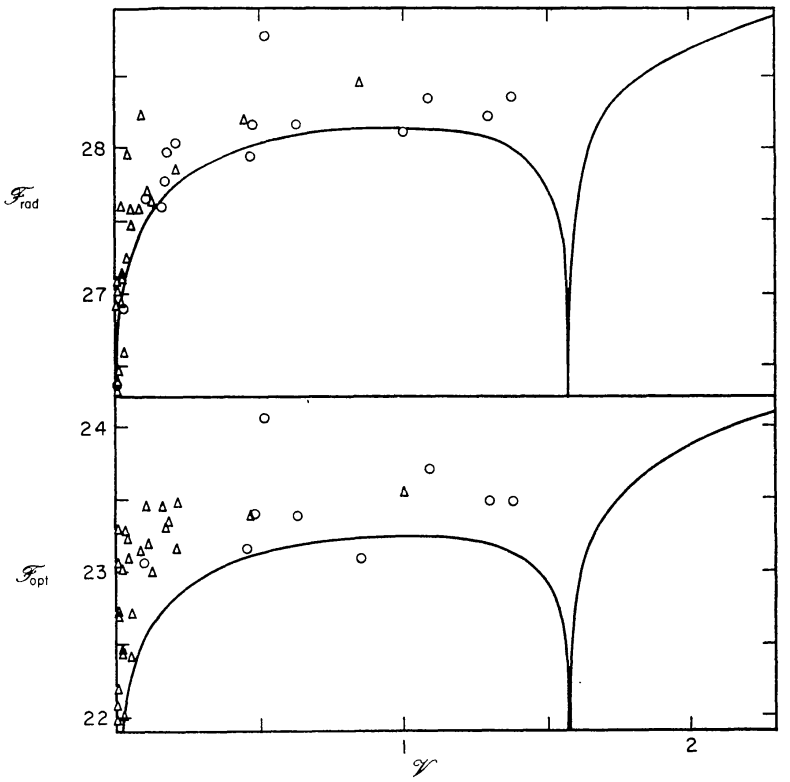

FIG. 4. *As in Fig.* 3, *but with* $\epsilon = 0{\cdot}1, \mathscr{F}_1 = 23{\cdot}15, \mathscr{F}_2 = 28{\cdot}05$.

Models corresponding to values of (Z_m, ϵ) outside the regions A, B, C of Fig. 2 are not consistent with the present data for quasars, unless the coordinate number-density of sources, or their luminosity, varies with epoch. Some examples are shown in Fig. 6: the sources in ranges of luminosity affected by selection effects have been omitted. The situation might change if the identifications of quasars in 3C are very incomplete and unrepresentative. But, for example, if all quasars with visual magnitude fainter than 18 are given a twin, to correct for the selection effect postulated by Penston & Rowan-Robinson (**12**), the regions of the $Z_m - \epsilon$ plane in which consistent models fall do not change significantly.

Thus a rather small range of models is consistent with the present data on the distribution of the quasars in space. Of these, three can also account for the anomalous 1·95 redshift:

$$Z_m = 2{\cdot}0, \quad \epsilon = 0{\cdot}0056 \quad \text{(for which } \chi(1{\cdot}95) = 2\pi)$$
$$Z_m = 2{\cdot}0, \quad \epsilon = 0{\cdot}14 \quad \text{(for which } \chi(1{\cdot}95) = \pi)$$

and

$$Z_m = 2{\cdot}95, \quad \epsilon = 0{\cdot}1.$$

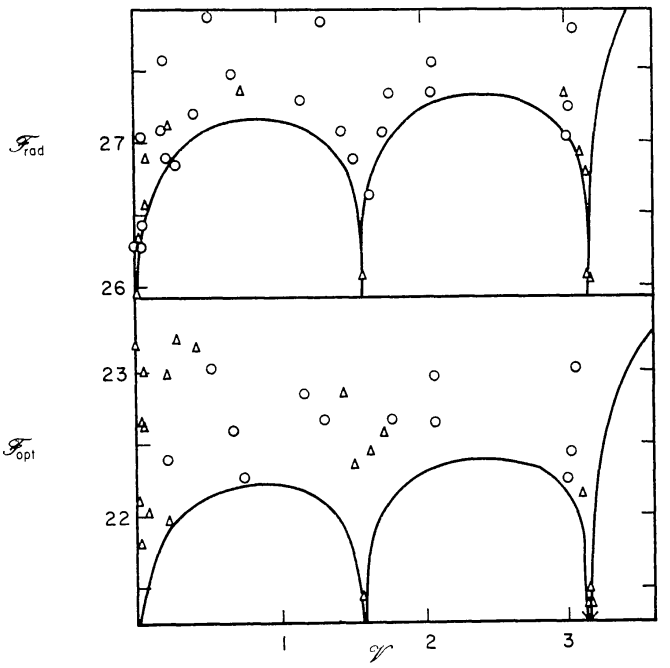

FIG. 5. *As in Fig.* 3, *but with* $Z_m = 2{\cdot}0$, $\epsilon = 0{\cdot}0056$, $\mathscr{F}_1 = 22{\cdot}35$, $\mathscr{F}_2 = 27{\cdot}25$.

For the latter model, Kardashev's argument would imply an optical depth of only 10^{-2} for objects with $z \simeq Z_m - 1$, so that it is hard to see how absorption lines could be produced.

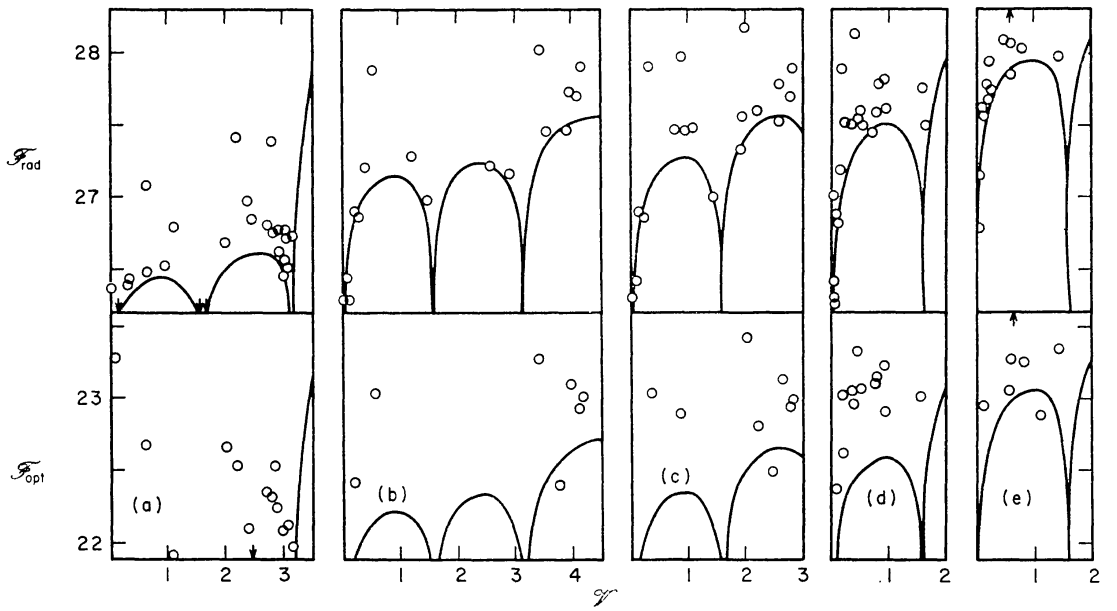

FIG. 6. *Distribution of radio and optical luminosities against volume (corrected for effects of optical and radio selection respectively) for the models:*

(a) $Z_m = 1{\cdot}5$, $\epsilon = 0{\cdot}00626$,
(b) $Z_m = 2{\cdot}0$, $\epsilon = 0{\cdot}001$,
(c) $Z_m = 2{\cdot}1$, $\epsilon = 0{\cdot}016$,
(d) $Z_m = 2{\cdot}262$, $\epsilon = 0{\cdot}068$,
(e) $Z_m = 2{\cdot}98$, $\epsilon = 0{\cdot}02$.

4.2 *Radio-galaxies.* In Ref. (4) the luminosity–volume test was applied to the radio-luminosities of the radio-galaxies in 3C, estimating the redshifts of those galaxies not yet measured from their estimated apparent visual magnitudes. Provided the latter magnitudes are not in error by more than ± 2, the distribution of the radio-galaxies in space is inconsistent with a wide range of cosmological models. The situation is not much altered for most of the cosmological models considered above. In fact, the only models found to be consistent with the present data for the radio-galaxies are those with an antipole at $z < 0{\cdot}45$, which requires $Z_m < 1{\cdot}5$ (from Fig. 2). For example the model with $Z_m = 1{\cdot}4$, $\epsilon = 0{\cdot}006$ is consistent with the distribution of the radio-galaxies and has $\chi(1{\cdot}95) = 2\pi$. However, it is highly inconsistent with the distribution of the quasars and gives an average density of the universe of $3{\cdot}6 \times 10^{-29}$ g cm^{-3}.

Fig. 7 shows the distribution of radio-luminosity against volume for 142 strong ($P \geqslant 10^{23{\cdot}5}$ w ster^{-1} (c/s)$^{-1}$) 3C radio-galaxies for the model $Z_m = 2{\cdot}0$, $\epsilon = 0{\cdot}0056$. Crosses denote galaxies whose redshifts have been measured, circles those whose redshifts have been estimated from

$$V = 20{\cdot}5 + 5 \log_{10} z + 5z \qquad (7)$$

where V is the estimated visual magnitude. Most galaxies whose redshifts are known satisfy this relation to within one magnitude and all to within two magnitudes. The continuous line shows the effect of the limiting 3C flux-level and the limitation $z \lesssim 0{\cdot}4$ imposed by the limiting visual magnitude of 20. The dotted line divides the

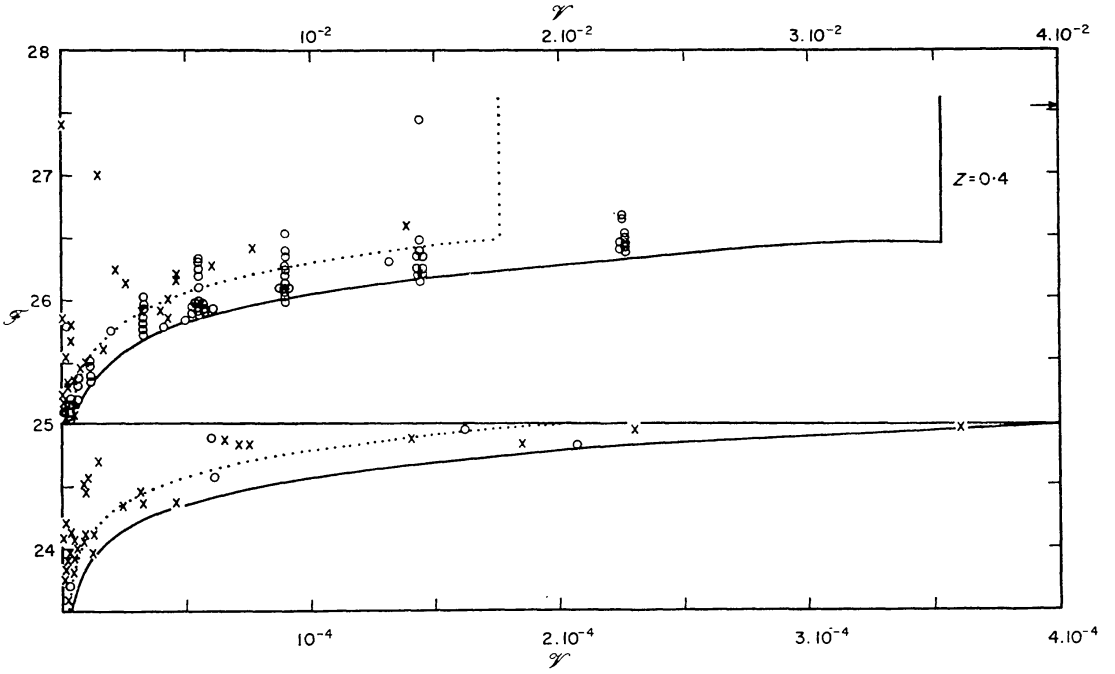

FIG. 7. *Distribution of radio-luminosity of 3C radio-galaxies against volume for the model with $Z_m = 2$, $\epsilon = 0{\cdot}0056$. Crosses denote galaxies whose redshifts are known, circles those whose redshifts have been estimated from equation (7). The upper volume scale refers to luminosities, $\mathscr{F} > 25$: the lower volume scale refers to $\mathscr{F} < 25$. The observable region is limited by the limiting 3C flux-level (continuous curve) and by the limiting optical magnitude of about 20 for galaxies (corresponding to $z \sim 0{\cdot}4$). The dotted curve divides the observable region in half at any given luminosity. The arrow to the right of the diagram denotes 3C 295, which has $V = 0{\cdot}11$ in this model.*

observable region in half at any given luminosity.* The number of radio-galaxies found in the near and further half of space are 61 and 80 respectively, and for sources with $P \geqslant 10^{25}$ w ster^{-1} (c/s)$^{-1}$, 39 and 69 respectively. The latter disposition has a probability of only 0·004 of occurring by chance. If all magnitudes are decreased by 2, these figures change to 65 : 76 and 39 : 54 (probability 0·1): but this is a very large systematic error to postulate.

This conclusion, that unless large errors exist in the present data no Lemaître model is consistent with the distributions in space of both quasars and radio-galaxies, should be contrasted with the result of introducing exponential evolutions into the more familiar models, where very similar rates of evolution were required for consistency with both quasars and radio-galaxies (**2**), (**4**). Of course, if evolutionary effects are now introduced into the Lemaître models, consistent models can be found: this may be necessary if the other evidence in favour of models with an antipole (**6**), (**9**) is confirmed by subsequent observations.

5. *Integrated radio background.* An important additional piece of evidence is the fact that at 178 Mc/s the integrated extragalactic radio background has a brightness temperature $T = 30 \pm 7°$ (**20**). If the coordinate number-density of sources having luminosity between P and $P+dP$ is $\eta(P)dP$, then

$$2KT\nu_0^2/c^2 = \int_0^\infty \eta(P)P\,dP \int_1^{\nu_b/\nu_0} Z^{-\alpha} R \frac{dr}{1+\frac{1}{4}kr^2}$$

where ν_0 is the frequency of observation, K is Boltzmann's constant and

$$P(\nu) \propto \nu^{-\alpha},\ \nu_0 \leqslant \nu \leqslant \nu_b,$$
$$= 0,\ \nu > \nu_b.$$

Thus

$$T = \frac{c^2}{2K\nu_0^2}(c/H_0)\overline{\eta P}.X(\alpha, \sigma_0, q_0) \tag{8}$$

where

$$\overline{\eta P} = \int_0^\infty \eta(P)P\,dP$$

and

$$X(\alpha, \sigma_0, q_0) = \int_1^{\nu_b/\nu_0} Z^{-\alpha} d(H_0 t).$$

X is a weighted age of the universe, where this age is reckoned in units of the Hubble time H_0^{-1}. This is illustrated by Fig. 8, which shows the loci in the $Z_m - \epsilon$ plane of models with equal age and with equal $X(0{\cdot}75, \sigma_0, q_0)$. The ratio of these quantities lies between 1 and 2 for most models considered in this paper.*

If $\alpha \geqslant 0$, $X < H_0 t_0$, which is finite if $\Lambda < \Lambda_c$ (even if $\nu_b \to \infty$). But if $\Lambda = \Lambda_c$ and $\nu_b/\nu_0 > Z_m$, then $Z^{-\alpha} > Z_m{}^{-\alpha}$ for all t, so that

$$X > \int_1^{Z_m} d(H_0 t),$$

which is divergent. Thus in the Eddington–Lemaître models ($\Lambda = \Lambda_c$), Olber's

* Actually these two loci are dependent on the spectral index of the sources: this has been taken into account in the computations. See, for example, Kafka (**18**).

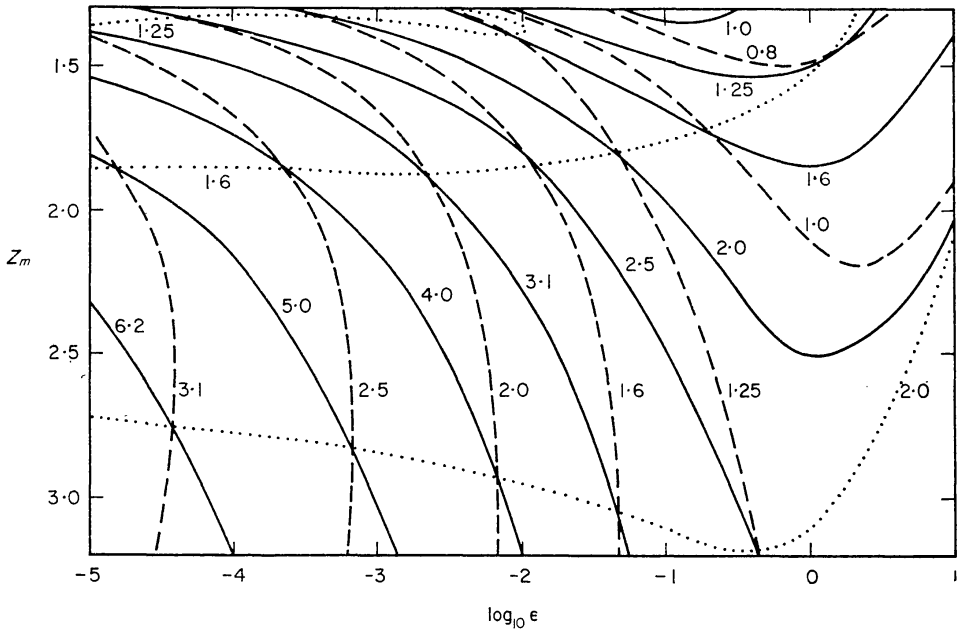

FIG. 8. *Z_m–ϵ, showing lines of constant H_0t_0 (continuous curves), X (broken curves) and H_0t_0/X (dotted curves). The temperature of the integrated extra-galactic radio background is proportional to X, which behaves like a weighted age of the universe.*

paradox is unresolved even though the universe is expanding (but is resolved by assuming sources radiated only for a finite time in the past).

If a dispersion in spectral indices is assumed, and the fraction of sources having spectral index between α and $\alpha+d\alpha$ is $\phi(\alpha)d\alpha$ (assumed independent of P and t), then

$$T = \frac{c^2}{2K\nu_0^2}(c/H_0)\overline{\eta P}.\bar{X}(\alpha_0, q_0) \tag{9}$$

where

$$\bar{X}(\alpha_0, q_0) = \int_{-\infty}^{\infty} X(\alpha, \sigma_0, q_0)\phi(\alpha)\, d\alpha$$

$$= \int_1^{\nu_b/\nu_0} d(H_0t) \int_{-\infty}^{\infty} Z^{-\alpha}\phi(\alpha)\, d\alpha.$$

The observed distribution (**13**) can be reasonably well represented by a Gaussian distribution, that is

$$\phi(\alpha) = (1/s\sqrt{2\pi}).\exp\{-(\alpha-\bar{\alpha})^2/2s^2\}$$

with $\bar{\alpha} = 0{\cdot}75$, $s = 0{\cdot}2$. Thus

$$\int_{-\infty}^{\infty} Z^{-\alpha}\phi(\alpha)\, d\alpha = Z^{-\bar{\alpha}+1/2s^2 \log_e Z}$$

and

$$\bar{X}(\alpha_0, q_0) = \int_1^{\nu_b/\nu_0} Z^{-\bar{\alpha}+1/2s^2 \log_e Z}\, d(H_0t).$$

The requirement that ν_b/ν_0 be finite is now essential to the resolution of Olber's paradox.

* Felten's calculation (**22**) of the energy density of starlight, in which he took $X \sim 1$, would have to be modified for the cosmological models considered here. The same applies to Veron's calculation (23) of the integrated extragalactic radio background.

In the de Sitter, Milne and Einstein–de Sitter models, $\bar{\chi}$ may be evaluated as a series of incomplete gamma-functions. For example, in the de Sitter model

$$\bar{X}(0, -1) = \int_1^{\nu_b/\nu_0} Z^{-\bar{\alpha}+1/2s^2 \log_e Z} dZ/Z$$

$$= \frac{1}{\bar{\alpha}} \int_0^x \exp(-y + \tfrac{1}{2}s^2y^2/2\bar{\alpha}^2) dy \qquad (10)$$

where $y = \bar{\alpha} \log_e Z$, $x = \bar{\alpha} \log_e \nu_b/\nu_0$

$$= \frac{1}{\bar{\alpha}} \int_0^x e^{-y} \left\{ \sum_{n=0}^{\infty} \frac{1}{n!} (s^2y^2/2\bar{\alpha}^2)^n \right\} dy$$

$$= \frac{1}{\bar{\alpha}} \sum_{n=0}^{\infty} \frac{1}{n!} (s^2/2\bar{\alpha}^2)^n \gamma(2n+1, x) \qquad (11)$$

where the incomplete Γ-function,

$$\gamma(a, x) = \int_0^x e^{-y} y^{a-1} dy.$$

So if $\bar{\alpha} = 0{\cdot}75$, $s = 0{\cdot}2$ and $\nu_b = 2 \times 10^5$ MHz, the first few terms give (**23**)

$$\bar{X}(0, -1) \simeq 1{\cdot}333\{0{\cdot}996 + 1{\cdot}60(s^2/2\bar{\alpha}^2) + 5{\cdot}64(s^2/2\bar{\alpha}^2)^2\}$$

$$= 1{\cdot}413.$$

whereas

$$X(\bar{\alpha}, 0, -1) = \frac{0{\cdot}996}{0{\cdot}75} = 1{\cdot}328.$$

Thus the error in assuming all sources to have the mean spectral index is considerably less than the uncertainties in $\overline{\eta P}$ and T. The situation is very similar for the Milne and Einstein–de Sitter models, except that $\bar{\alpha}$ should be replaced in equations (10) and (11) by $\bar{\alpha}+1$ and $\bar{\alpha}+3/2$, respectively. In the remainder of this paper we shall neglect the effect of the dispersion in spectral indices.

The application of the luminosity–volume test described in Section 4.2 above showed that for the radio-galaxies $\eta(P)$ was not independent of redshift for models with $Z_m \geqslant 1{\cdot}5$. Nevertheless the mean value of $\eta(P)$ over the observable volume of space can be estimated in each model and the corresponding integrated background predicted. For 'weak' radio-galaxies, i.e. those with luminosities less than $10^{23{\cdot}5}$ w ster^{-1} (c/s)$^{-1}$ at 178 MHz, the luminosity function of Caswell & Wills (**14**) can be used, since $\eta(P)$ is practically independent of cosmological model for such sources.

The quantity $(c/H_0)\overline{\eta P}$, which is independent of H_0, depends only slightly on cosmological model. It is practically independent of ϵ, is a slowly decreasing function of Z_m and is of the order of

$$13 . 10^{-23} \text{ w m}^{-2} \quad \text{for} \quad 1{\cdot}4 \leqslant Z_m \leqslant 3{\cdot}0, \; 10^{-5} \leqslant \epsilon \leqslant 1.$$

Slightly over half this figure is contributed by weak radio-galaxies: the contribution of the quasars is negligible, about $0{\cdot}5 \times 10^{-23}$ w m^{-2}. Radio-wise, it is reasonable to regard the quasars as a subclass of the radio-galaxies, visible at large redshift by virtue of exceptionally large optical emission. From this point of view it is not necessary to include their contribution to $\eta(P)$.

Now $c^2/2K\nu_0^2 = 10^{23{\cdot}01}$ deg m^2 w^{-1} so $T \sim 13\bar{X}°$. The dependence of T on model is shown more precisely in Fig. 9. The models in the regions B and C (see

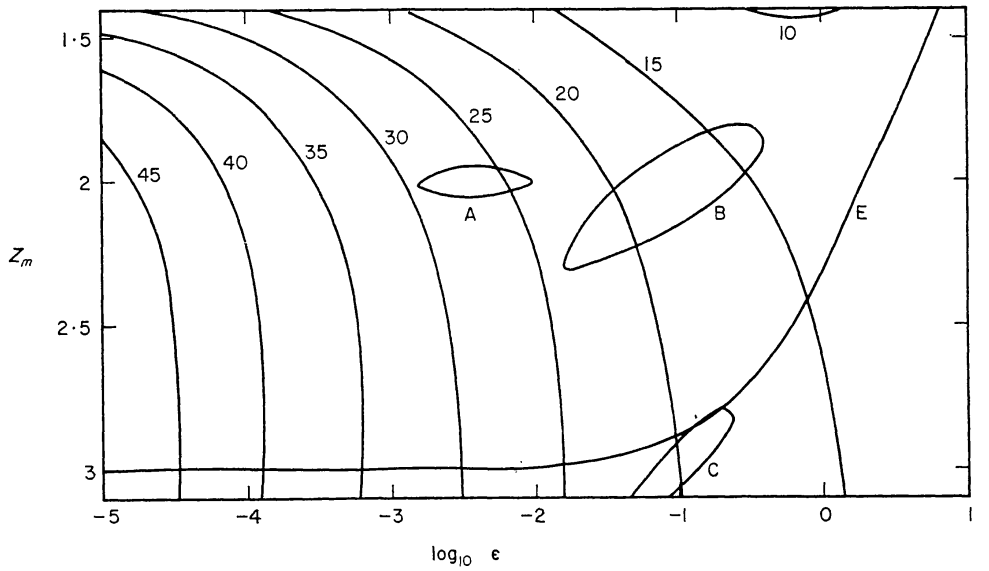

FIG. 9. *Z_m–ϵ, showing lines of constant integrated extra-galactic background temperature at 178 MHz. Models in the region A fall in the observed range $30\pm7°$. The curve labelled E corresponds to $\sigma_0 = 0{\cdot}05$, or $\rho_0 = 10^{-30}\,g\,cm^{-3}$.*

Section 4.1) give rather low background temperatures, in the range 15–20°. The models in the region A fall within the strip corresponding to the observed values $30\pm7°$ (**20**). Comparing this strip with Fig. 8, the corresponding ages of the universe are in the range 2–$4(H_0^{-1})$. The model proposed by Kardashev gives a background temperature at 178 MHz of 46°, in the absence of evolutionary effects.

The strip of models consistent with the observed integrated background could change very drastically if evolutionary effects are introduced. For consistency of the Kardashev model with the distributions in space of radio-galaxies and quasars, the number-density or luminosity of sources should increase with redshift in the range $0<z<0{\cdot}5$, and decrease in the range $1<z<2$.

6. *Number-counts to low flux-level.* In calculating the theoretical number-count relationship for models with antipoles, both Kardashev (**7**) and McVittie & Stabell (**8**) have neglected the contribution of sources in the vicinity of epochs such that $\chi(z) = \pi, 2\pi, 3\pi$ etc. This, however, is incorrect. Suppose $\chi(z_n) = n\pi$, $n = 1, \ldots, N$, and that the values of z for which sources of luminosity P and spectral index are observed to have flux-level S are given by $z = z_n \pm \beta_n$, $n = 1 \ldots N$ and $z = \beta_0$.

Let the corresponding values of χ be $n\pi \pm \delta_n$, and δ_0. Then if

$$\delta_n \ll 1,\ D(z_n \pm \beta_n) \simeq R_0 Z_n \delta_n,$$

so

$$S = P/R_0^2 Z_n^{1+\alpha} \delta_n^2.$$

Also

$$V(z_n \pm \beta_n) \simeq \tfrac{1}{2} n\pi \pm \delta_n^3/3.$$

The number of sources brighter than S is proportional to

$$R_0^3\{\nu(\beta_0) + \sum_{n=1}^{N} [V(z_n+\beta_n) - V(z_n-\beta_n)]\} = 1/3\left(\delta_0^3 + 2\sum_1^N \delta_n^3\right) R_0^3$$

$$= 1/3(P/S)^{1.5}\left\{1 + 2\sum_1^N Z_n^{-3(1+\alpha)/2}\right\}$$

$$= 1/3(P/S)^{1.5}\xi \text{ say.}$$

Kardashev and McVittie & Stabell, assumed that $\xi \simeq 1$, but in fact, for the Kardashev model, $Z_1 = 2{\cdot}84117$, $Z_2 = 2{\cdot}94829$, $Z_3 = 3{\cdot}02076$, $Z_4 = 4{\cdot}92604$ (Kardashev has different values for Z_3 and Z_4 as a consequence of his incorrect expression for Q: see Section 3.1 above), and so $\xi = 1{\cdot}355$. Moreover, as $\epsilon \to 0$ the number of solutions of $\chi(z) = n\pi$ with $1 + z \simeq Z_m$ tends to infinity, so $\xi \to \infty$.

Fig. 10 shows the exact log N–log S relation for sources of luminosity 10^{25} w ster^{-1} (c/s)$^{-1}$, for three models with antipoles and also the relations obtained when the observed dispersion in luminosity is taken into account. These theoretical log N–log S curves are very much less steep than that observed at 178 MHz. This failure to account for the radio source-counts to low flux-level applies to all models within the range considered in this paper: $1{\cdot}4 \leqslant Z_m \leqslant 3{\cdot}0$; $10^{-5} \leqslant \epsilon \leqslant 1$.

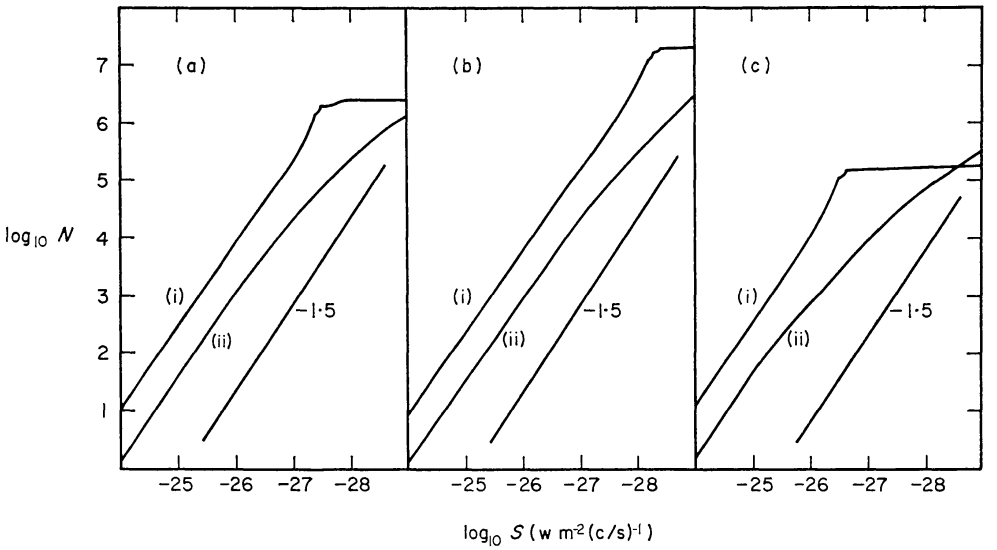

FIG. 10. log N–log S *curves at* 178 *MHz* (*i*) *for sources with luminosity* 10^{25} *w ster*$^{-1}$ (*c/s*)$^{-1}$ *and coordinate number density* 10^6 $(c/H_0)^{-3}$, (*ii*) *for the observed distribution of luminosities, for three models. Lines of slope* $-1{\cdot}5$ *are shown in each case.*

(*a*) $Z_m = 2{\cdot}0$, $\epsilon = 0{\cdot}0056$
(*b*) $Z_m = 2{\cdot}95$, $\epsilon = 0{\cdot}00002$
(*c*) $Z_m = 1{\cdot}4$, $\epsilon = 0{\cdot}006$.

Conclusions

(i) A small range of models is consistent with the distribution in space of 3C quasars, including three models that might also explain the anomalous absorption redshift of 1·95: $(Z_m, \epsilon) = (2{\cdot}0, 0{\cdot}0056)$, $(2{\cdot}0, 0{\cdot}14)$ and $(2{\cdot}95, 0{\cdot}1)$.

The first of these gives an integrated background temperature at 178 MHz for extragalactic sources of 26°, in agreement with the observed value of $30 \pm 7°$ and provides a natural explanation of the absence of 3C quasars with redshift greater than 2·2. The average density of the universe in this model is about $5 . 10^{-30}$ g cm^{-3}, requiring the existence of an appreciable quantity of intergalactic or intercluster material.

(ii) For consistency with the distribution in space of 3C radio-galaxies, it is necessary that an antipole occur at $z \leqslant 0{\cdot}45$. It would then be the most remarkable coincidence that the galaxy identified with 3C295, with $z = 0{\cdot}46$, satisfies the Hubble relation (**21**). Very large systematic errors must be present in the data for

models with $Z_m \geqslant 1{\cdot}5$ to be consistent with the distribution of 3C radio-galaxies, without the introduction of evolutionary effects.

(iii) None of the models considered in this paper predict source-count curves as steep as that observed. Evolutionary effects have to be introduced and there seems no reason for preferring models with an antipole to the more familiar models with $\Lambda = 0$, unless further evidence (confirmation of the anomalous absorption redshift, or of the correlation of radio-sources in opposite directions in the sky) points towards them. The interpretation of the radio source-counts to low flux-level in terms of exponential evolutionary effects will be discussed in a subsequent paper.

Acknowledgments. The computing was performed by the Computer Centre Staff, Queen Mary College, to whom thanks are due for helpful assistance. I am grateful to a referee, and to Dr R. Stabell, for comments that enabled this paper to be improved.

Queen Mary College,
Mile End Road,
London E.1.
1968 *May.*

References

(1) Rees, M. J. & Sciama, D. W., 1967. *Nature, Lond.*, **213,** 374.
(2) Rowan-Robinson, M., 1968. *Mon. Not. R. astr. Soc.*, **138,** 445.
(3) Schmidt, M., 1968. *Astrophys. J.*, **151,** 393.
(4) Rowan-Robinson, M., 1967. *Nature, Lond.*, **216,** 1289.
(5) Petrosian, V., Salpeter, E. & Szekeres, P., 1967. *Astrophys. J.*, **147,** 1222.
(6) Shklovsky, I., 1967. *Astrophys. J.*, **150,** L1.
(7) Kardashev, N., 1967. *Astrophys. J.*, **150,** L135.
(8) McVittie, G. C. & Stabell, R., 1967. *Astrophys. J.*, **150,** L141.
(9) Solheim, J. E., 1968. *Nature, Lond.*, **217,** 41.
(10) Burbidge, G. R. & Burbidge, E. M., 1967. *Astrophys. J.*, **148,** 107.
(11) Wagoner, R. V., 1967. *Astrophys. J.*, **149,** 465.
(12) Penston, M. V. & Rowan-Robinson, M., 1967. *Nature, Lond.*, **213,** 375.
(13) Long, R. J., Smith, M. A., Stewart, P. & Williams, P. J. S., 1966. *Mon. Not. R. astr. Soc.* **134,** 371.
(14) Caswell, J. L. & Wills, D., 1967. *Mon. Not. R. astr. Soc.*, **135,** 231.
(15) Oort, J. H., 1958. Solvay Conference on *La Structure et l'Evolution de l'Univers*, p. 163.
(16) Humason, M. L., Mayall, N. U. & Sandage, A. R., 1956. *Astr., J.*, **61,** 97.
(17) Tinsley, B. M., 1967. Ph.D. Thesis, University of Texas.
(18) Kafka, P., 1967. Max-Planck Institute für Physik und Astrophysik, München, preprint.
(19) Veron, P., 1967. *Ann. d'Astrophys.*, **30,** 719.
(20) Bridle, A. H., 1967. *Mon. Not. R. astr. Soc.*, **136,** 219.
(21) Sandage, A. R., 1965. *Astrophys. J.*, **141,** 1560.
(22) Felten, J. E., 1966. *Astrophys. J.*, **144,** 241.
(23) Pearson, K., 1922. *Tables of the Incomplete Gamma-Function*, London.